Long term Geomagnetically Induced Current Observations from New Zealand: Peak Current Estimates for Extreme Geomagnetic Storms

Craig J. Rodger, and Daniel H. Mac Manus

Department of Physics, University of Otago, Dunedin, New Zealand

Michael Dalzell

Transpower New Zealand Limited, New Zealand

Alan W. P. Thomson, and Ellen Clarke

British Geological Survey, United Kingdom

Tanja Petersen

GNS Science, New Zealand

Mark A. Clilverd

British Antarctic Survey (NERC), Cambridge, United Kingdom

Tim Divett

Department of Physics, University of Otago, Dunedin, New Zealand

Main point # 1: Analysis of a 14 year dataset of GIC in a transformer in Islington, New Zealand, shows peaks correlated with local H' .

Main point # 2: Peak GIC values are very poorly correlated with global geomagnetic indices (ap, Kp, Aa*), and weakly correlated with local ak index values.

Main point # 3: Estimated peak GIC at Islington for a 100 year return period geomagnetic storm is ~155-605 A, and ~155-910 A for 200 years.

Abstract. Geomagnetically Induced Current (GIC) observations made in New Zealand over 14 years show induction effects associated with a rapidly varying horizontal magnetic field (dB_H/dt) during geomagnetic storms. This study analyses the GIC observations in order to estimate the impact of extreme storms as a hazard to the power system in New Zealand. Analysis is undertaken of GIC in transformer number six in Islington, Christchurch (ISL M6), which had the highest observed currents during the 6 November 2001 storm. Using previously published values of 3000 nT/min as a representation of an extreme storm with 100 year return period, induced currents of ~455 A were estimated for Islington (with the 95% confidence interval range being ~155-605 A). For 200 year return periods using 5000 nT/min, current estimates reach ~755 A (confidence interval range 155-910 A). GIC measurements from the much shorter dataset collected at transformer number 4 in Halfway Bush, Dunedin, (HWB T4), found induced currents to be consistently a factor of three higher than at Islington, suggesting equivalent extreme storm effects of ~460-1815 A (100 year return) and ~460-2720 A (200 year return). An estimate was undertaken of likely failure levels for single phase transformers, such as HWB T4 when it failed during the 6 November 2001 geomagnetic storm, identifying that induced currents of ~100 A can put such transformer types at risk of damage. Detailed modeling of the New Zealand power system is therefore required put this regional analysis into a global context.

1. Introduction

The most intense geomagnetic storm ever recorded [*Cliver and Svalgaard*, 2004], now known as the Carrington Event, followed a white light solar flare in September 1859 [*Carrington et al.*, 1859]. Should a storm of similar intensity occur today, technological systems around the world are expected to be severely affected. According to some scenarios, a future occurrence of an extreme geomagnetic storm of magnitude similar to the Carrington storm would cause widespread failure of electric power networks on regional scales due to the impact of Geomagnetically Induced Currents (GIC). Lately a number of popular scientific articles have been published about the growing realization that GIC pose a potential risk to our technological societies [e.g, *Kelleher*, 2016; *Witze*, 2016], and the new policy and strategic planning which is coming from that realization [e.g., *MacAlester and Murtagh*, 2014; *National Science and Technology Council*, 2015]. It should be noted that GIC are one of a wide range of Space Weather impacts which occur during extreme storms, some of which have been described as "extraordinary" [*Knipp et al.*, 2016; *Love and Coïsson*, 2016].

A United States National Academy of Sciences (NAS) report [*Baker et al.*, 2008] indicated that the most extreme geomagnetic storms could destroy 300 or more of the 2,100 high-voltage transformers that are the backbone of the U.S. electric grid. The academy's report noted that replacements for transformers might not be available for a year or more, and the cost of damage in the first year after a storm could be as high as USD$2 trillion [*Baker et al.*, 2008; *JASON*, 2011]. It should be noted that economic impacts of such extreme events are difficult to estimate [e.g., *Oughton et al.*, 2017], with another study suggesting 20-40 million people would be affected for 16 days to ~2 years creating a total financial impact to the USA of USD$0.6-2.6 trillion [*Lloyd's*, 2013]. Similar levels of economic global supply chain disruption ($0.5-2.7 trillion) have been estimated due to the impact on the US electrical transmission network of differing extreme geomagnetic storm scenarios [*Oughton et al.*, 2016]. Clearly, it is widely agreed that the impact of an extreme geomagnetic storm would be substantial, while the wider uncertainties make establishing the specific technological and economic impact highly challenging.

Large GICs are usually closely associated with geomagnetic field disturbances that have a high rate of change ($d\mathbf{B}/dt$) and in particular the rate of change of the magnetic component in the horizontal direction [*Mäakinen*, 1993; *Viljanen*, 1998, *Bolduc et al.*, 1998]. In the current study we represent the rate of change of the magnetic horizontal component, dB_H/dt, by H'. Recently, a ~14 year record of GIC measured in multiple transformers in New Zealand were contrasted with geomagnetic field variations, confirming that for the majority of locations the best correlation was clearly with H' [*Mac Manus et al.*, 2017]. The primary argument for considering the time derivative of the magnetic field is that it is a good indicator of the expected magnitude of the geomagnetically induced electric field on the Earth's surface [*Cagniard*, 1953], which is the primary driver of GICs [e.g., *Viljanen et al.*, 2001].

There have been a number of fairly large geomagnetic storms in the last decades, in particular March 1989, November 2001 and October 2003. However, the historical record demonstrates more extreme geomagnetic storms can occur, for example those of September 1859 or May 1921, which may have been ~10 times larger than occurred in March 1989 [*Hutchins and Overbye*, 2011]. It has been suggested that there is a 6-7% probability of an 1859-type solar storm in the next 10 years [*Love*, 2012; *Cannon et al.*, 2013], corresponding to a recurrence period of 138-162 years. These values correspond to a ~27-30% probability in the next 50 years. Extreme space weather events are low-frequency, high-risk phenomena and as such, are necessarily studied through statistical methods. A large range of probabilities regarding the recurrence of another Carrington level storm have been reported (spanning ~3-12% [*Riley*, 2012; *Kataoka*, 2013]), likely due to differing statistical approaches. This is well demonstrated by the finding that the probability of a Carrington storm occurring in the next 10 years ranges from 3% for a log-normal distribution to 10.3% for a power-law distribution

[*Riley and Love*, 2016]. There are also large uncertainties associated with these extreme event analyses. While *Love* (2012) indicated that the most likely occurrence of an 1859-type solar storm with 10 year return period is 6.3% they also reported that the 68.3% confidence range for 10 year return is 1.6-13.7%.

When contrasted with major seismic events, the likelihood of another significant Carrington-level geomagnetic storm is reasonably high. For example, there is a ~14% chance of a very large earthquake (magnitude>7) on the New Zealand Alpine Fault in the next 50 years [*Berryman et al*., 2012], corresponding to a recurrence period of ~330 years. The Alpine Fault is one of the longest, straightest, and fastest-moving plate boundary transform faults on Earth and poses a substantial seismic hazard to the country of New Zealand. In contrast an extreme geomagnetic storm would not only effect New Zealand, but would likely have global consequences.

Across the world there has been increasing interest in understanding the potential impact of GIC on electrical networks in order to mitigate the potential hazards. One example is a recent GIC research consortia operating across Europe, looking at European hotspots, providing monitoring and looking at the worst case scenarios [*EURISGIC*, 2013]. Multiple countries are now investigating the hazards to the electrical network [*Beck*, 2013], focusing on large to extreme storms.

To the best of our knowledge, the largest GIC reported to date is 269 A measured at Simpevarp-2 in Southern Sweden on 6 April 2000 [*Wik et al.,* 2008], which was associated with a magnetic field rate of change of only ~200 nT/min at the nearest magnetic observatory (Uppsala). This rate of change is large, but not particularly extreme. The Hydro Quebec collapse in 1989 has been associated with a substorm-linked *H'* of 479 nT/min [*Fiori et al.*, 2014], although the largest rate of change ever reported was ~2000 nT/min in the lower Baltic [*Kappenman*, 2004]. The latter event occurred on 13-14 July 1982 where disturbances of ≥2000 nT/min were measured in central and southern Sweden, coincident with geo-electric field readings of 9.1 V/km and were associated with tripping of transformers and lines [*Wik et al.*, 2009]. During May 1921 in the same region geo-electric fields of ~20 V/km are thought to have occurred, suggesting peak magnetic field changes of ≥4000 nT/min [*Kappenman*, 2004].

At mid and low-latitudes, large GIC have been related to storm sudden commencements and sudden impulses, rather than substorms [e.g., *Watari* et al., 2009 (Japan); *Marshall et al.*, 2012 (New Zealand); *Marshall et al.*, 2013 (Australia); *Carter et al.*, 2015 (geomagnetic equator)]. This has been discussed in more detail by *Fiori et al.* [2014]. One example of a significant GIC impact in this latitude range is the destruction of a transformer at Dunedin/Halfway Bush (HWB T4), New Zealand. This occurred on 6 November 2001 at 1:53 UT, within a few minutes of a storm sudden commencement. That event has been described qualitatively in the scientific literature [*Béland and Small*, 2004], and was subsequently analyzed in detail [*Marshall et al.*, 2012].

Clearly, indicative values of extreme geomagnetic field changes are required to consider the impact of extreme storms and GIC magnitudes. *Thomson et al.* [2011] used extreme value statistics (EVS) and one-minute data from 28 European magnetic observatories over 30 years and found that peak *H'* increased with geomagnetic latitude, with a distinct maximum in levels between ~53-62º latitude. This study concluded that across 55-60º geomagnetic latitude the estimated 100 year return period maxima for *H'* is 1000-4000 nT/min, while the 200 year values range from 1000-6000 nT/min (with the range representing 95% confidence). These maximum *H*' values should be contrasted with the "reasonable worst case scenario" of 5000 nT/min considered for the United Kingdom grid [*Canon et al.*, 2013].

In this study we investigate GIC observations made in New Zealand during 14 years of significant geomagnetic storms. Our focus in this work is to consider how large storms can be used to estimate the impact of extreme storms as a GIC hazard in New Zealand. As GIC are closely linked to the rate of change of the horizontal magnetic field component we focus on the time periods with significant *H'*, and examine how these events contrast with global and local disturbance indices. We focus on measurements made at transformer number 6 in Islington, Christchurch (ISL M6), which had the highest observed currents during the 6 November 2001 storm [*Marshall et al.*, 2012; *Mac Manus et al.*, 2017]. This allows us to estimate likely GIC magnitudes expected for this location during extreme storms. By contrasting GIC measurements from the much shorter dataset collected at HWB T4, we estimate a GIC "danger level" for that style of single phase transformer.

2. Experimental Datasets

2.1 New Zealand GIC Observations

A detailed description of the New Zealand GIC measurements in the South Island has been previously reported [*Mac Manus et al.*, 2017]. The following section is a brief summary, and the reader is directed to the earlier study for a more complete explanation.

Transpower New Zealand Limited has measured DC currents in multiple South Island transformers. Near continuous archived DC current data exist since 2001, initially starting with 12 different substations, and gradually expanding from 2009 to include 17 substations. The more recent expansion in measurement locations, from about 2013 onwards, were driven by an increasing interest in monitoring potential Space Weather impacts. This later expansion incorporated the Halfway Bush substation, including the replacement number 4 transformer (HWB T4, location shown by the red star in Figure 1) one phase unit of which was written off due to the effect of GIC on 6 November 2001 [*Béland and Small*, 2004]. Over the time period 2001-2015 a total of 61 distinct transformers have been monitored using Hall effect current transducers (Liaisons Electroniques-Mécaniques (LEM) model LT 505-S). The primary purpose for the DC observations is monitoring stray currents when the high voltage DC link between the South and North Islands operates in single wire earth return mode or with unbalanced currents on the conductors. *Marshall et al.* [2012] has previously described DC observations from the LEM sensors during the 6 November 2001 storm.

The process by which this dataset is corrected to remove stray earth return currents and any calibration offsets was given in detail by *Mac Manus et al.* [2017]. Once these return currents, which can be >10 A in some locations, were removed, a substantial GIC dataset was produced. For some transformers this corresponds to a nearly continuous set of GIC measurements from 2002-2015. One example is the number 6 transformer in Islington (ISL M6), the location of which is shown by the yellow star in Figure 1. As noted before, ISL M6 measured the highest observed currents during the 6 November 2001 storm, peaking at ~33 A [*Mac Manus et al.*, Fig. 5, 2017]. As ISL M6 experiences rather large GIC magnitudes and has measurements over a long time period, we focus on it in the current study. In addition, we note that as shown in Figure 1 the Islington substation is close to the Eyrewell magnetic observatory, described below. All the GIC observations reported here are after the corrections described in *Mac Manus et al.* [2017] have been undertaken.

2.2 Magnetometer

The location of the magnetometer station at Eyrewell (EYR) is shown in Figure 1 as a blue hexagon. EYR is part of INTERMAGNET (http://www.intermagnet.org/) and is operated by GNS Science, New Zealand. This station provides 1 min (and for some periods higher time resolution) magnetic field data with coordinates *X* (positive to geographic north), *Y* (positive to the east), and *Z* (positive vertically downwards) to the INTERMAGNET collaboration, with a resolution of 0.1 nT. Absolute magnetic field measurements are provided by a DI-fluxgate magnetometer and a proton precession magnetometer. The 1-minute resolution magnetic field observations are constructed from higher time resolutions samples by applying a Gaussian filter centred on the minute and calculating the mean, following the INTERMAGNET guidelines. One minute mean values are only calculated when 90% or more of the values required for calculation of the mean are available. When fewer than 90% of the required values are available, the one minute value is flagged as missed. As discussed later in the paper the highest time resolution available has changed with time.

The magnetic horizontal component, *H*, were determined from the North (*X*) and East (*Y*) components in the usual way (i.e., $H=\sqrt{X^2+Y^2}$) and the rate of change of the horizontal component, *H'*, from $d(\sqrt{X^2+Y^2})/dt$.

3. Large *H'* events from New Zealand-regional observations

As noted earlier, it has been previously reported that GIC magnitudes are linked to the rate of change of the magnetic component in the horizontal direction. For the New Zealand region, *Mac Manus et al.* [2017] found that the time variation of South Island GIC was typically well correlated with *H'* measured by the Eyrewell magnetic observatory. In order to study the occurrence and properties of GIC in New Zealand, we investigate periods in which large |*H'*| values were observed at Eyrewell. We limit ourselves to the time period from 2001-2015 in which there are archived GIC measurements, and set a threshold of 40 nT/min in the one-minute resolution EYR |*H'*| observations to represent "large" rates of change. This value is somewhat arbitrary, to provide an event list of reasonable size. Only one event was allowed per UT day, represented by the peak |*H'*| value for that time period. The resulting list was then manually checked to remove any events produced by data errors, which affected two potential events. This process produced 31 events, the times of which are listed in Table 1, ordered by decreasing |*H'*|.

Note that the first event listed in Table 1 is at 1:52 UT on 6 November 2001, which is the most significant |*H*|'-value observed by the New Zealand magnetic observatory from 2001-2015. As has been previously mentioned this is also the time of the most significant space weather impact suffered in the New Zealand electrical network. While *Béland and Small* [2004] and *Marshall et al.* [2012] both report on operational procedures put in place to manage the risk of GIC to the New Zealand grid, from 2001 to date a similarly sized event has yet to affect the South Island. In addition to the New Zealand rank number, peak |*H'*| value and UT time, Table 1 also lists the associated geomagnetic indices (aa* ranking, Kp, ap, and the EYR ak-index, each of which describe various variations in the geomagnetic field) and GIC observations for these events Note that we have used the traditional format for reporting Kp values on the "scale of thirds". Some readers may be more familiar with the alternative format, where 9- is given as 8.7, 8+ as 8.3, and 8o as 8. *aa** is the 8-point (or 24-hour) running average of the 3-hour *aa* index [*Clilverd et al.*, 2002]. This filters out longitudinal differences and enables a simple index, based on only two measurement points to be representative of global activity, whilst at the same time retaining the 3-hour time resolution. The *aa** rank value is the ordered rank of the storm and is based on the maximum *aa** reached in that storm. For 6 events of the 31 (4, 15, 17, 20, 24, and 29) there were no GIC observations from ISL M6. All of these events occurred in 2001 when the archiving of the South Island DC observations were inconsistent, and thus ~20% of the large |*H'*| disturbances across the ~15 year window have been lost. This leaves us with 25 distinct examples of New Zealand large |*H'*| disturbances for which we have ISL M6 GIC observations.

3.1 Contrast with Global Index Values

Table 1 includes a number of different geomagnetic indices against each one of the *H'* events. Most are global indices (e.g., aa* rank, Kp, and ap), while the EYR K-index is local to the Eyrewell magnetometer. It is well known that the "global" indices can be more or less biased to different parts of the world depending on the magnetic observatory data used to determine them. Of the global indices, this should be less of an issue for the aa* index, as this is made up of only 2 stations, one in the northern hemisphere and the other in the southern hemisphere, approximately antipodal from one another. In contrast the Kp and ap indices are created from observations by 13 observatories, 2 in the southern hemisphere (Australia and New Zealand), and 11 in the northern hemisphere (7 in Europe, 4 in North America) [*Mayaud*, 1980]. This is likely to explain the relatively poor correlation between the global index values and the peak |*H'*| value observed in New Zealand.

The upper two panels of Figure 2 show a comparison between the EYR-reported peak |*H'*| values and the ap (upper panel) and Kp (middle panel) for all 25 events considered. It is particularly clear from the middle panel that there is a poor "by eye" correlation between global magnetic field disturbances measured by the Kp index and EYR local peak |*H'*| value observed in New Zealand. Kp is both quantized and non-linear, and hence a linear fit is not particularly valuable. In contrast, the ap index is a linear index and thus we examine the coefficient of determination (r^2) to test the quality of a linear correlation between ap and EYR-reported peak |*H'*|. However, r^2 is only 0.39, demonstrating a low-quality relationship. As noted above, this may be partly explained by the contrast of global indices derived from non-uniformly spread observatories with the local South Island magnetometer measurements which are best correlated with local GIC observations [*Mac Manus et al.*, 2017]. Consistent with this idea we see from Table 1 the largest peak |*H'*| value of 190.8 nT/min at 1:52 UT on 6 November 2001 was associated with a Kp of 8.7 and ap of 300 nT, while event 10 at 18:36 UT on 20 November 2003 has the same Kp/ap values but a EYR peak |*H'*| value of 78 nT which is ~2.4 times smaller than on 6 November.

One might expect the aa* index to better correlate with EYR peak |*H'*|, as this is a global measure which is less spatially biased, with the Southern Hemisphere observatory located comparatively close to New Zealand in Canberra, Australia. Table 1 shows the aa* ranking of geomagnetic storms from 2001-2015 associated with each of our 25 events. However, once again, the global index is a poor predictor of the local peak |*H'*| values. Event 1 was globally ranked as the 7th largest aa* storm (aa*=152 nT), with event 10 ranked 2nd (aa*=250 nT) and event 20 ranked 4th (aa*=216 nT). While the Halloween storm in October 2003 is the highest ranked aa* storm (aa*=333 nT) and is associated with events 2 and 3, it is worth noting that event 2 with peak EYR |*H'*| of 170.6 nT/min occurred for the global Kp value of 7.7, while the smaller event 3 with peak EYR |*H'*| of 166.2 nT/min happened during the more globally intense period with a global Kp value of 9.0.

While it is not scientifically unexpected for the GIC-driving local geomagnetic field variations to be fairly poorly correlated with global geomagnetic indices, this is an important message to stress to the electrical industry who are becoming increasingly Space Weather conscious. It is not uncommon to find the industry players focused on the internet-available global geomagnetic index values and forecasts. This is also the case in New Zealand with the Transpower procedures for managing GIC [*Transpower*, 2015] requiring a geomagnetic storm to be G2 or greater on the NOAA Space Weather scale (equivalent to Kp=6) before investigating generation and transmission constraints and G3 or great (equivalent to Kp=7) before advising the duty operations manager. The poor correlations in Figure 2 suggests that the link between the Kp index values and the local magnetic field changes which drive GIC is fairly poor, in line with other published work, such that other approaches might need to be considered in order to create an effective warning system or “GIC danger” level.

3.2 Contrast with Local Index Values

One alternative option would be to rely on warnings from the local New Zealand magnetic observatory. *Mac Manus et al.* [2017] reported that the time variation in observed GIC was typically well correlated with *H'*, as expected. The lower panel of Figure 2 shows a comparison between the EYR-determined ak-index value and the EYR-peak |*H'*| values. In this case there is a better "by eye" agreement between the two parameters, which is unsurprising given they are determined from the same fundamental observations. The coefficient of determination (r^2) in this case has a value of 0.59, suggesting a weak correlation. The highest 3-hourly K-index values from EYR do not correspond to the highest peak |*H'*| values, likely due to the large time window over which the ak-indices are determined relative to *H'*. One might suggest that near real time *H'* warnings may assist Transpower during large geomagnetic storms. At this time EYR observations are available with a ~1 hour delay, but there are plans to decrease this to 10 min. While that information could be useful during a GIC event, in practice Transpower already has realtime information on GIC at their control centers from the LEM units, and more value would come from forecasting of likely GIC activity. New Zealand is located at mid-geomagnetic latitudes where the large |*H'*| values tend to be linked to sudden commencements and sudden impulses [*Fiori et al.*, 2014] that occur at the beginning of geomagnetic storms, hence making accurate prediction more challenging. Significant additional research is required in this area in order to allow useful warnings of mid-latitude GIC. This is part of an international-scale scientific problem at the heart of contemporary Space Weather work.

4. Case Study: 29 October 2003

The largest Space Weather event with the most significant New Zealand GIC impact occurred on 6 November 2001. However this event has been described in detail in the existing literature, both in terms of its technical impact [*Béland and Small*, 2004; *Marshall et al.*, 2012], and the GIC measurements that occurred both at ISL M6 and also across other South Island sites [*Marshall et al.*, 2012; *Mac Manus et al.*, 2017]. The later study specifically examined the correlation between the time variation of the GIC measured at ISL M6 and the EYR *H'* values for this storm, reporting they were fairly strong (r^2=0.71). Table 1 includes the magnitude of the GIC observed at ISL M6 for this event (33.1 A). These values are the peak current reported within ±2 min of the EYR-peak |*H'*| values to allow for varying levels of induction and changes in the driving field.

However, it is apparent from the next columns values in Table 1 that the relationship between the EYR *H'* values and the peak ISL M6 GIC magnitude is not directly linear. While the EYR-peak $|H'|$ values decrease slowly across the first three events (i.e., 190.8, 170.2, and 166.2 nT/min) the peak ISL M6 GIC magnitude behaves very differently (33.1, 21.1, and 34.1 A). As is immediately obvious, the largest GIC measurement at ISL M6 across the 25 events occurred on 29 October 2003. Peak currents occurred at 06:12 UT, shortly after a storm sudden commencement at 06:11 UT. Figure 3 shows the time variation of the ISL M6 GIC observations on 29 October 2003. The timing of the 06:11 UT sudden commencement is marked with a heavy magenta line, which clearly coincides with the beginning of significant GIC activity. A second, slightly smaller GIC peak (22.3 A), is also marked in this Figure at 19:21 UT.

One possible, and simple, explanation for the different scaling relationships between the EYR-peak $|H'|$ values and peak ISL M6 GIC magnitudes seen across the first three events in Table 1 is differing time resolution between the data. Other possible explanations are modifications in the electrical grid topology from event to event, or variations in the direction of the magnetic field change in the horizontal plane giving rise to different E_x and E_y fields that depend on the conductivity structure. Here we examine the first, and simplest, explanation.

The peak $|H'|$ values come from the 1 min resolution EYR observations. In contrast, the time resolution of the GIC data for the Halloween Storm period (Table 1 events 2 and 3) was ~10 s, such that faster variations in $|H'|$ might cause different responses in the GIC. We explore this by examining 5 s time resolution EYR measurements which were available for that storm period (this was the highest EYR time resolution at that time). Figure 4 contrasts the time variation of the $|H'|$ values from the 60 s (upper panel) and 5 s (lower panel) resolution data. In both cases the rate of the change of the H-component is shown with the same units of nT/min. For the 60 s resolution data the 06:11 UT sudden commencement has a peak $|H'|$ value of 166.2 nT/min, while the $|H'|$ value at the time of the second pulse of GIC seen at 19:21 UT in Figure 3 was 86.7 nT/min. In contrast the ~06:11 UT sudden commencement has a peak |*H′*| value of 583.1 nT/min in the 5 s resolution data, with the ~19:21 UT value being 434.3 nT/min. The ratio of the first and second GIC peaks is ~1.53 (i.e., 34.1/22.3), which is more similar to the ratio of 1.34 between the corresponding peaks in the 5 s resolution data, rather than those for the 60 s data, which is 1.92. In addition, the higher time resolution |*H′*| values have a more similar time variation to that seen in the GIC measurements (Figure 3), suggesting that the higher time resolution magnetic field measurements are better at capturing the driving of the GIC.

5. Comparison between 60 s and 5 s resolution *H′* values

Mac Manus et al. [2017] examined the correlation between the time variations of the geomagnetic fields and the GIC observations. We now examine the correlation between the peak GIC magnitudes at the ISL M6 transformer and the peak |*H′*| values for the 25 events described previously. As a starting point we make use of the one minute EYR magnetometer data, as this is available for all 25 events. A plot of the GIC magnitudes against 60 s resolution peak |*H′*| values is shown by the blue crosses in Figure 5. A linear fit is shown by the red dashed line. The coefficient of determination (r^2) is 0.71, suggesting a fairly strong correlation, although there is still significant scatter. It seems unlikely that this is due to the distance from the Islington substation to the EYR magnetic observatory, as this is only ~12 km. The scatter might in part be due to the use of 60 s resolution magnetic field data, which we consider in the next section.

Following on from the results of the case study presented in Section 4, we investigate the relationship between the ISL M6 GIC and the available higher time resolution *H′* values. The available information is summarized in Table 2. While one minute EYR magnetometer observations have always been available, across the 2001-2015 time window various levels of higher time resolution measurements have sometimes been collected. These are 20 s, 5 s, and 1 s resolution data. Generally only one level of higher time resolution measurements have been available at a given time, although in some rare cases there have been two (e.g., for the storm on 15 May 2005 at 8:17 UT, both 5 s and 20 s are available in addition to the 60 s resolution observations.

The higher time resolution data provide some explanation for the observed ISL M6 GIC responses. As was detailed in Section 4, the 5 s *H′* peak values for events 2 and 3 appear to better explain the magnitudes of the ISL M6 GIC. Event 16 (11 Sep 2005 5:37 UT) also supports using the value of higher resolution magnetic field observations to investigate peak GIC magnitude. Here the *H′* value of ~295 nT/min is very similar to that for event 2 (~298 nT/min), as are the GIC magnitudes (19.2 A c.f., 21.1 A). However, this apparent pattern is at least partially confounded by event 5 (18 Feb 2003 5:08 UT), where both the 60 s and 5 s resolution *H′* peak values would imply a larger GIC than that observed. Nonetheless, as is shown in Figure 6, typically the higher resolution *H′* values predict the GIC magnitudes at ISL M6 better than the one minute value do. While we are restricted to only 13 events, due to data availability, there is a significantly improved r^2 value of 0.88 seen for the fit in Figure 6 when compared to that for Figure 5 (r^2=0.71). Note that moving to even higher time resolution magnetometer observations leads to very poor correlations. As can be seen from Table 2 the 1 s resolution *H′* peak values do not seem to relate well to the GIC, confirmed by the extremely poor r^2 value of 0.08 for the associated linear fit. This most likely reflects noise problems with the EYR 1 s observations used to derive the rates of change, rather than a sudden transition in the fundamental physics on this time scale.

Although the changing geomagnetic field is the fundamental driver of the GIC, the GIC are caused by the induced geo-electric field. While the geo-electric field is determined from the rates of change of the magnetic field through Faraday's Law, the geo-electric field depends on both the electrical structure of the Earth and the time history of the changing magnetic field, not the immediate value of *dB/dt*. As such there can be phase lags between the changing magnetic field and peak GIC levels; from fundamental physical theory such offsets will vary depending on the frequency variations in the driving magnetic field and the varying penetration of these time varying fields into the Earth.

6. Extrapolation to Extreme Storms

The goal of this study is to provide an estimate of the maximum GIC which might be expected in New Zealand transformers during an extreme geomagnetic storm. In a general sense this style of question is best answered through modeling studies [e.g., *Beggan et al.*, 2013; *Kelly et al.*, 2017], and at this point such a model is being developed for New Zealand, to be validated by the South Island GIC measurements. Nonetheless, the work presented in the preceding sections of the current study allows some preliminary estimates to be made. We follow similar studies undertaken using 30 years of European magnetic observatories [*Thomson et al.*, 2011], as many of these lie at similar geomagnetic latitudes to New Zealand (particularly those in the United Kingdom). *Thomson et al.* [2011] concluded that the estimated 100 year return period maxima for H' is 1000-4000 nT/min, while the 200 year return period values range from 1000-6000 nT/min (with the range representing 95% confidence). Following the United Kingdom estimate for an extreme event of 5000 nT/min [*Cannon et al.*, 2013] we use 3000 nT/min and 5000 nT/min as an initial representation of extreme storms with 100 and 200 year return periods, respectively, but take the 95% confidence interval range as an indication of the possible span.

6.1 ISL M6 Extreme Storm Estimates

Figure 7 linearly extrapolates the fitted line of ISL M6 GIC magnitudes from Figure 5 to $|H'|$ values that cover the extreme storm range. In this figure the estimated peak GIC at ISL M6 for two suggested representations of a 100 year return period storm are shown in magenta, while the red stars and current values are for the representations of a 200 year return period storm. As the differences between the various H' extreme storm representations are large, there are also significant differences in the GIC estimates. For a 100 year return period geomagnetic storm the peak GIC predicted for ISL M6 is 455 A, while for a 200 year return period geomagnetic storm this is 755 A. If we use the full 95% confidence interval range of 1000-4000 nT/min reported by *Thomson et al.* [2011] for a 100 year return period storm the peak GIC predicted for ISL spans 153-605 A. This should be contrasted with the *Thomson et al.* [2011] 95% confidence interval range for a 200 year return period storm of 1000-6000 nT/min, leading to GIC spanning 153-907 A. The confidence interval ranges are shown by the ringed points in Figure 7. Such a large range emphasizes the large uncertainties associated with extreme event analysis.

Again, we note that these results should be re-examined once a model is produced and validated to predict GIC in New Zealand.

6.2 HWB T4 Extreme Storm Estimates

Since 2012 GIC has been monitored at HWB T4, the location of the transformer written off after the 6 November 2001 storm (event 1 in Table 1). As might be expected by the sensitivity shown by HWB to the 6 November 2001 event, the currents observed at HWB T4 during significant geomagnetic storms are large; in most cases the GIC observed in Dunedin and specifically Halfway Bush are the largest of all the measuring locations across the South Island. An example of this was shown by *Mac Manus et al.* [Fig. 7, 2017] for a storm on 2 October 2013. The observed GIC peaked at 1:56 UT (event 9 in Table 1), with the HWB T4 GIC nearly reaching 49 A, in contrast to the ~19 A at ISL M6.

Generally, the GIC at HWB T4 are considerably larger than those at ISL M6. Table 1 includes the HWB T4 GIC magnitudes for the five events for which measurements were being made at that transformer, as well as the ratio between the GIC at HWB T4 and ISL M6. For most events (4 of the 5) there is a fairly consistent ratio between the GIC magnitudes at the two locations, ranging from 2.6-3.3 with a mean of 2.9 and median of 2.85. The exception is event 25 (22 Jun 2015 18:34 UT) for which it is clear that the HWB

T4 current measurements failed to capture the peak of the ~2 min spike at the start of the event, while the ISL M6 data does capture this spike. For the remainder of the 16 hour period for which there was significant GIC present, the HWB T4 observations were ~3 times larger than ISL M6 (not shown) consistent with the other 4 events.

On the basis of these observations we suggest that there is consistently an approximate factor of 3 between the HWB T4 and ISL M6 GIC, such that the currents expected during extreme storms will be ~3 times larger at HWB T4 than at ISL M6. Using the extrapolation shown in Figure 7 would therefore predict that for a 100 year return period geomagnetic storm the peak GIC predicted for HWB T4 spans from ~460-1815 A (using the 95% confidence interval range), while for a 200 year return period geomagnetic storm this is ~460-2720 A. At this point the reason for the factor of three difference between the GIC observed at the two different transformer locations is unclear. It likely depends upon network layout and electrical properties, and the varying ground conductivity, and will be one of the questions we hope to answer through the modeling studies we have now started.

6.3 Hazard Estimates

While the extreme storm GIC magnitudes discussed above are clearly rough estimates, albeit based on empirical evidence, the size of these currents are concerning. They are very large, and it seems like they will produce failures in the South Island grid. As is evident from the scientific literature, it is unclear what level of GIC will produce difficulties or failure of transformers. In most cases the transformers which form the backbone of electrical networks are built to order, with significant differences from transformer to transformer. Nonetheless, we can use the New Zealand observations to estimate the peak GIC at HWB T4 when this transformer failed on 6 November 2001 (event 1 of Table 1). While GIC were not monitored at HWB T4 at this time, the peak GIC at ISL M6 was measured as 33.1 A. As the HWB T4 GIC are typically ~3 times those at ISL M6 this suggests the one of the single phase transformers making up HWB T4 failed at ~100 A. While 100 A appears a fairly low value compared to the very large GIC values we found for extreme storms, this estimate is similar to another already in the literature. Modeling of the GIC experienced at the large step-up transformer which failed at the Salem Nuclear Power Plant during the Hydro Quebec storm of March 1989 suggested the maximum GIC at that time was ~95 A [*Kappenman*, Fig 4-8, 2010], close to the maximum possible for a transformer of this design [*Girgis and Ko*, 1992]. Note, however, that the 100 A value is only a rather rough indication of the level at which a transformer may be damaged in a rapid event. Much more detailed analysis is required to understand the transformer response to given GIC amplitudes and waveforms. In addition, it has been suggested that multiple exposures to comparatively low levels of GIC can lead to degradation and subsequent failure [*Moodley and Gaunt*, 2017], without a single large GIC event.

Based on Table 1 it is tempting to conclude that the highest GIC risk in the South Island electrical network is to transformers in Dunedin. However, while rather large GIC have been observed there during the geomagnetic storms of the last years, a comprehensive modeling study (or more comprehensive measurements) are needed to establish where the largest currents are occurring. Nonetheless, New Zealand seems to experience higher GIC than other island countries located at mid-latitudes. It may be that New Zealand's comparatively sparse electrical network with long distances between substations contributes to the higher GIC levels. During the 30 October 2003 severe geomagnetic storm, the measured and modeled GIC magnitudes in the Scottish part of the UK grid exceeded ~40 A [*Thomson et al.*, 2005]. The largest currents seen during two years of GIC observations from Hokkaido, Japan was ~4 A [*Watari et al.*, 2009], with modeling suggesting the maximum GIC expected at this location for the 6 November 2001 storm would have been ~15 A [*Pulkkinen et al.*, 2010].

7. Summary and Discussion

In this study we have focused on GIC observations available from 2001-2015 at the number 6 transformer in the Islington substation (Christchurch, New Zealand). Our goal has been to better understand the properties of GIC at this location, which was the site of the largest measured currents during New Zealand's most significant space weather event to date, such that estimates can be made of the GIC expected for extreme storms.

We have shown that:

1. The highest rate of change of the horizontal component of the magnetic field (H') observed in New Zealand magnetometer data across these 15 years was on 6 November 2001, at the time of the most serious Space Weather impact to the South Island electrical grid.

2. The size of the New Zealand H' values correlates poorly to global geomagnetic indices (ap, Kp, and aa* rank). While it is clear that our large H' values occur during geomagnetic storms that are significant on a global scale, the New Zealand H' values are not well linked to the global intensities.

3. The size of the New Zealand H' values are better linked to the local geomagnetic activity index, the Eyrewell magnetic observatory K values. However, there is no direct correlation between these parameters, likely due to the very different time scales on which activity is measured.

4. In general, the peak GIC magnitude reported from ISL M6 shows a good correlation (r^2=0.71) with the magnitude of the New Zealand H' values derived from 60 s resolution observatory data.

5. In some cases the ISL M6 peak GIC magnitudes are better explained by H' values determined from higher resolution observatory data. In general, there is a strong correlation (r^2=0.88) between ISL M6 GIC and 5 s resolution H' values. We suggest that monitoring of

the high time resolution *H'* values would be of value to the New Zealand grid operator, Transpower Ltd.

6. We consider two approaches for determining the likely peak GIC at ISL M6 for extreme geomagnetic storms. Using *H*' values with a time resolution of 60 s the peak GIC predicted for a 100 year return period geomagnetic storm of~455 A was estimated (with the 95% confidence interval range being ~155-605 A). For 200 year return periods using 5000 nT/min, current estimates reach ~755 A (confidence interval range 155-910 A). The large ranges in these peak GIC values come from the large range in suggested extreme storm *H*' values.

7. Peak GIC at transformer number 4 of the Halfway Bush substation (HWB T4, Dunedin, New Zealand) tends to be ~3 times larger than those observed at ISL M6. As such the extreme storm GIC will be ~3 times larger than those given in point 6, i.e., maximum values for a 100 year return period storm of 1815 A, and a 200 year return period maximum of 2720 A.

8. Based on the failure of HWB T4 during the storm of 6 November 2001, the risk level for this transformer is ~100 A, similar to some other estimates for other transformers in the literature.

The size of the peak GIC we have estimated for extreme geomagnetic storms at HWB T4 is significantly higher than those recently reported for potential maximum values in the United Kingdom network. *Beggan et al.* [2013] suggested that the maximum GIC in one network node (equivalent to a substation) was 460 A for a 200 year return level storm, while *Kelly et al.* [2017] suggested an extreme "Carrington level" storm lead to a maximum computed node value of 832 A. One assumes that the substation corresponding to the node will include more than one transformer, and the current will be distributed amongst those transformers, making the comparison more extreme. Nonetheless our estimate is based on an extrapolation from experimental observations. While the estimates and analysis in this study are specific to New Zealand, they should be relevant to GIC investigations in other mid-latitude locations. It may be that the New Zealand network structure and ground conductivity makes the South Island more vulnerable than the United Kingdom. We are currently undertaking modeling studies to explore this, which will be reported in a future paper.

Acknowledgments. This research was supported by the New Zealand Ministry of Business, Innovation & Employment Hazards and Infrastructure Research Fund Contract UOOX1502. The authors would like to thank Transpower New Zealand for supporting this study.

Data availability is described at the following websites: http://www.intermagnet.org/imos/imos-list/imos-details-eng.php?iaga_code=EYR (Eyrewell magnetometer). K indices for Eyrewell are available by contacting one of the coauthors, Tanja Petersen (T.Petersen@gns.cri.nz). The New Zealand LEM DC data from which we determined GIC measurements were provided to us by Transpower New Zealand with caveats and restrictions. This includes requirements of permission before all publications and presentations. In addition, we are unable to directly provide the New Zealand LEM DC data or the derived GIC observations. Requests for access to the measurements need to be made to Transpower New Zealand. At this time the contact point is Michael Dalzell (Michael.Dalzell@transpower.co.nz). We are very grateful for the substantial data access they have provided, noting this can be a challenge in the Space Weather field [*Hapgood and Knipp,* 2016]. The Kp and ap data came from the World Data Centre for Solar-Terrestrial Physics, Chilton, UK (https://www.ukssdc.ac.uk/wdcc1/geophy_menu.html), the aa* data from British Geological Survey (http://www.geomag.bgs.ac.uk/data_service/data/magnetic_indices/aaindex.html).

References

Baker, D. N., et al. (2008), Severe Space Weather Events: Understanding Societal and Economic Impacts, 144 pp., National Academies Press, Washington, D. C., USA.

Beck, C. (2013), The International E-Pro™ Report: International Electric Grid Protection, Electric Infrastructure Security Council, EIS Council, Washington D.C, September, 2013.

Beggan, C. D., D. Beamish, A. Richards, G. S. Kelly, and A. W. P. Thomson (2013), Prediction of extreme geomagnetically induced currents in the UK high-voltage network, Space Weather, 11, 407–419, doi:10.1002/swe.20065.

Béland, J., and K. Small (2004), Space weather effects on power transmission systems: The cases of Hydro-Québec and Transpower New Zealand Ltd, in Effects of Space Weather on Technological Infrastructure, edited by I. A. Daglis, pp. 287–299, Kluwer Acad., Netherlands.

Berryman, K.R., U. A. Cochran, K. J. Clark, G. P. Biasi, R. M. Langridge, and P. Villamor, (2012), Major earthquakes occur regularly on an isolated plate boundary fault, *Science, 336,* 1690-1693, doi:10.1126/science.1218959.

Bolduc, L. (2002), GIC observations and studies in the Hydro-Québec power system, Journal of Atmospheric and Solar-Terrestrial Physics, 64, 1793 – 1802.

Cagniard, L. (1953), Basic theory of the magnetotelluric method of geophysical prospecting, Geophysics, 18, 605—635, doi:10.1190/1.1437915.

Cannon, P., M. Angling, L. Barclay, C. Curry, C. Dyer, R. Edwards, G. Greene, M. Hapgood, R. B. Horne, D. Jackson, C. N. Mitchell, J. Owen, A. Richards, C. Rodgers, K. Ryden, S. Saunders, M. Sweeting, R. Tanner, A. Thomson, and C. Underwood (2013), Extreme space weather: impacts on engineered systems and infrastructure, Royal Academy of Engineering, London.

Carrington, R. C. (1859), Description of a Singular Appearance Seen in the Sun on September 1, 1859, Mon. Not. Roy. Astron. Soc., 20, 13-15.

Carter, B. A., E. Yizengaw, R. Pradipta, A. J. Halford, R. Norman, and K. Zhang (2015), Interplanetary shocks and the resulting geomagnetically induced currents at the equator, Geophys. Res. Lett., 42, 6554–6559, doi:10.1002/2015GL065060.

Cliver, E. W., and L. Svalgaard (2004), The 1859 Solar–Terrestrial Disturbance and the Current Limits of Extreme Space Weather Activity, Solar Physics, 224: 407, doi:10.1007/s11207-005-4980-z.

Clilverd, M. A., T. D. G. Clark, E. Clarke, H. Rishbeth, and T. Ulich, The causes of long-term change in the aa index, J. Geophys. Res., 107(A12), 1441, doi:10.1029/2001JA000501, 2002.

EURISGIC (2013), European Risk from Geomagnetically Induced Currents. European Union Framework Seven consortium project. Details available from http://www.eurisgic.eu/ (downloaded 31 March 2015).

Fiori, R. A. D., Boteler, D. H., and Gillies, D. M. (2014), Assessment of GIC risk due to geomagnetic sudden commencements and identification of the current systems responsible, Space Weather, 12(1), 76–91.

Girgis, R. S., and C. D Ko (1992), Calculation Techniques and Results of Effects of GIC Currents as Applied to Two Large Power Transformers, IEEE Trans. Power Delivery, 7(2), DOI:10.1109/61.127070, April 1992.

Hapgood, M., and D. J. Knipp (2016), Data Citation and Availability: Striking a Balance Between the Ideal and the Practical, Space Weather, 14, 919–920, doi:10.1002/2016SW001553.

Hutchins, T. R., and T. J. Overbye (2011), The effect of geomagnetic disturbances on the electric grid and appropriate mitigation strategies, North American Power Symposium (NAPS), doi: 10.1109/NAPS.2011.6025162.

JASON (2011), Impacts of severe space weather on the electric grid, Rep. JSR-11-320, MITRE Corp., McLean, Va. [Available at https://fas.org/irp/agency/dod/jason/space-weather.pdf]

Kappenman, J. (2010), Geomagnetic Storms and Their Impacts on the U.S. Power Grid, Metatech Corporation, Goleta, Calif. [Available at https://fas.org/irp/eprint/geomag.pdf]

Kappenman, J. G. (2004), The Evolving Vulnerability of Electric Power Grids, Space Weather, 2: n/a. doi:10.1029/2003SW000028.

Kataoka, R. (2013), Probability of occurrence of extreme magnetic storms, Space Weather, 11, 214–218, doi:10.1002/swe.20044.

Kelleher, S. (2016), Space weather gains national and international attention, Eos, 97,doi:10.1029/2016EO045115. Published on 8 February 2016.

Kelly, G. S., A. Viljanen, C. D. Beggan, and A. W. P. Thomson (2017), Understanding GIC in the UK and French high-voltage transmission systems during severe magnetic storms, Space Weather, 15, doi:10.1002/2016SW001469.

Knipp, D. J., et al. (2016), The May 1967 great storm and radio disruption event: Extreme space weather and extraordinary responses, Space Weather, 14, 614–633, doi:10.1002/2016SW001423.

Lloyd's (2013), Solar Storm Risk to the North American Electric Grid: A Lloyds Space Weather Study, available online from http://www.lloyds.com/~/media/Lloyds/Reports/Emerging%20Risk%20Reports/Solar%20Storm%20Risk%20to%20the%20North%20American%20Electric%20Grid.pdfJASON (2011), Impacts of Severe Space Weather on the Electric Grid (JSR-11-320), The MITRE Corporation, McLean, Virginia, USA.

Love, J. J. (2012), Credible occurrence probabilities for extreme geophysical events: Earthquakes, volcanic eruptions, magnetic storms, Geophysics Research Letters, 39, L10301, doi:10.1029/2012GL051431.

Love, J. J., and P. Coïsson (2016), The geomagnetic blitz of September 1941, Eos, 97, doi:10.1029/2016EO059319. Published on 15 September 2016.

Mäakinen, T. (1993), Geomagnetically induced currents in the Finnish power transmission system, Finn. Meteorol. Inst. Geophys. Publ., 32.

Mac Manus, D. H., C. J. Rodger, M. Dalzell, A. W. P. Thomson, M. A. Clilverd, T. Petersen, M. M. Wolf, N. R. Thomson, and T. Divett (2017), Long term Geomagnetically Induced Current Observations in New Zealand: Earth return Corrections and Geomagnetic Field Driver, Space Weather, 15, doi:10.1029/2017SW001635, (in press).

MacAlester, M. H., and W. Murtagh (2014), Extreme Space Weather Impact: An Emergency Management Perspective, Space Weather, 12, 530–537, doi:10.1002/2014SW001095.

Marshall, R. A., et al. (2013), Observations of geomagnetically induced currents in the Australian power network, Space Weather, 11, 6–16, doi:10.1029/2012SW000849.

Marshall, R. A., M. Dalzell, C. L. Waters, P. Goldthorpe, and E. A. Smith (2012), Geomagnetically induced currents in the New Zealand power network, Space Weather, 10, S08003, doi:10.1029/2012SW000806.

Mayaud, P. N., (1980), Derivation, Meaning, and use of geomagnetic indices, Geophysical Monograph 22, American Geophysical Union.

Moodley, N., and C. T. Gaunt (2017), Low Energy Degradation Triangle for power transformer health assessment, IEEE Trans. Dielectrics Electrical Insulation, 24(1), 639 - 646, doi:10.1109/TDEI.2016.006042

National Science and Technology Council (2015), National space weather strategy, 14 pp., White House Off. of Sci. and Technol. Policy, Washington, D. C.

Oughton, E. J., A. Skelton, R. B. Horne, A. W. P. Thomson, and C. T. Gaunt (2017), Quantifying the daily economic impact of extreme space weather due to failure in electricity transmission infrastructure, Space Weather, 15, doi:10.1002/2016SW001491.

Oughton, E.; Copic, J.; Skelton, A.; Kesaite, V.; Yeo, Z. Y.; Ruffle, S. J.; Tuveson, M.; Coburn, A. W.; and Ralph, D. (2016), Helios Solar Storm Scenario; Cambridge Risk Framework series; Centre for Risk Studies, University of Cambridge

Pulkkinen, A., Kataoka, R., Watari, S., and Ichiki, M. (2010), Modeling geomagnetically induced currents in Hokkaido, Japan, Advances in Space Research, 46(9), 1087-1093.

Riley P., and J.J. Love (2016), Extreme Geomagnetic Storms: Probabilistic Forecasts and their Uncertainties, Space Weather, 14, doi:10.1002/2016SW001470.

Riley, P. (2012), On the probability of occurrence of extreme space weather events, Space Weather, 10, S02012, doi:10.1029/2011SW000734.

Thomson, A. W. P., A. J. McKay, E. Clarke, and S. J. Reay (2005), Surface electric fields and geomagnetically induced currents in the Scottish Power grid during the 30 October 2003 geomagnetic storm, Space Weather, 3, S11002, doi:10.1029/2005SW000156.

Thomson, A. W., Dawson, E. B., and Reay, S. J. (2011), Quantifying extreme behavior in geomagnetic activity, Space Weather, 9(10).

Transpower (2015), Manage geomagnetic induced currents, Rep. PR-DP-252/V05-03, Syst. Oper. Div., Wellington.

Viljanen, A., Relation of Geomagnetically Induced Currents and Local Geomagnetic Variations, IEEE Trans. Power Delivery, 13, 1285–1290, 1998.

Viljanen, A., Nevanlinna, H., Pajunpää, K., and Pulkkinen, A. (2001), Time derivative of the horizontal geomagnetic field as an activity indicator. Annales Geophys., 19, 1107–1118.

Watari, S., Kunitake, M., Kitamura, K., Hori, T., Kikuchi, T., Shiokawa, K., Nishitani, N., Kataoka, R., Kamide, Y., Aso, T., Watanabe, Y., and Tsuneta, Y. (2009), Measurements of geomagnetically induced current in a power grid in Hokkaido, Japan, Space Weather, 7, S03002, doi:10.1029/2008SW000417.

Wik, M., A. Viljanen, R. Pirjola, A. Pulkkinen, P. Wintoft, and H. Lundstedt (2008), Calculation of geomagnetically induced currents in the 400 kV power grid in southern Sweden, Space Weather, 6, S07005, doi:10.1029/2007SW000343.

Wik, M., R. Pirjola, H. Lundstedt, A. Viljanen, P. Wintoft, and A. Pulkkinen (2009), Space weather events in July 1982 and October 2003 and the effects of geomagnetically induced currents on Swedish technical systems, Ann. Geophys. 27, 1775-1787.

Witze, A. (2016), US sharpens surveillance of crippling solar storms, Nature 537, 458–459, doi:10.1038/537458a. Published on 22 September 2016.

Ellen Clarke, and Alan W. P. Thomson, British Geological Survey, The Lyell Centre, Research Avenue South, Edinburgh EH4 4AP, United Kingdom. (email: awpt@bgs.ac.uk, ecla@bgs.ac.uk)

Mark A. Clilverd, British Antarctic Survey (NERC), High Cross, Madingley Road, Cambridge CB3 0ET, England, U.K. (e-mail: macl@bas.ac.uk).

Michael Dalzell, Transpower New Zealand Ltd, 96 The Terrace, PO Box 1021, Wellington, New Zealand. (email: Michael.Dalzell@transpower.co.nz).

Tim Divett, Daniel H. Mac Manus, and Craig J. Rodger, Department of Physics, University of Otago, P.O. Box 56, Dunedin, New Zealand. (email: tim.divett@otago.ac.nz, macda381@student.otago.ac.nz, crodger@physics.otago.ac.nz).

Tanja Petersen, GNS Science, 1 Fairway Drive, Avalon, Lower Hutt 5011, New Zealand (email: T.Petersen@gns.cri.nz).

#	Peak Time [UT]	Peak $\lvert H' \rvert$ [nT/min]	aa* rank	ap [2 nT]	Kp	EYR ak [nT]	ISL M6 GIC [A]	HWB H4 GIC [A]	Ratio
1	6 Nov 2001 1:52	190.8	7	300	9-	480	33.1	-	-
2	31 Oct 2003 5:36	170.6	1	179	8-	480	21.1	-	-
3	29 Oct 2003 6:11	166.2	1	400	9o	480	34.1	-	-
4	24 Nov 2001 5:56	115.3	8	56	5+	160	-	-	-
5	18 Feb 2003 5:08	109.4	19	56	5+	160	12.5	-	-
6	15 May 2005 8:17	97.9	17	236	8+	480	15	-	-
7	8 Nov 2004 7:12	90.2	3	236	8+	800	14.9	-	-
8	29 May 2003 22:09	88.7	4	236	8+	160	14.3	-	-
9	2 Oct 2013 1:56	85.6	68	56	5+	96	19.1	48.8	2.6
10	20 Nov 2003 18:36	78	2	300	9-	800	12.1	-	-
11	10 Nov 2004 2:42	74.9	3	179	8-	280	14.2	-	-
12	4 Nov 2003 6:27	73.9	3	94	6+	160	13	-	-
13	17 Mar 2015 4:46	68.6	6	39	5-	96	17	47.9	2.8
14	23 Apr 2002 4:49	66.9	289	39	5-	96	11.1	-	-
15	25 Sep 2001 23:15	64.7	64	154	7+	160	-	-	-
16	11 Sep 2005 5:37	62.6	14	132	7o	160	19.2	-	-
17	22 Oct 2001 1:36	60.8	16	132	7o	160	-	-	-
18	21 Jan 2005 23:18	60.3	26	154	7+	160	8	-	-
19	26 Jul 2004 22:50	57.6	5	154	7+	280	18.6	-	-
20	31 Mar 2001 4:34	57.5	4	300	9-	280	-		-
21	5 Dec 2004 7:47	56.8	382	32	4+	96	8.6	-	-
22	17 Mar 2013 6:01	54.3	44	111	7-	96	13.2	43.9	3.3
23	24 Oct 2003 15:25	52.5	81	111	7-	96	7.3	-	-
24	11 Apr 2001 21:41	51.4	12	236	8+	160	-	-	-
25	22 Jun 2015 18:34	51.2	15	236	8+	480	12.2	12.8	1.0
26	17 Apr 2002 11:07	47.8	22	80	6o	96	6.5	-	-
27	12 Sep 2014 15:55	43.3	105	48	5o	54	9.8	28.6	2.9
28	9 May 2003 7:43	42.7	70	48	5o	96	4.6	-	-
29	13 Apr 2001 10:42	42.4	12	154	7+	160	-	-	-
30	18 Mar 2002 13:23	41.6	206	48	5o	54	5.9	-	-
31	26 Sep 2011 19:38	40.6	46	94	6+	14	8.7	-	-

Table 1. Properties of the time periods where the rate of change of the horizontal component of the magnetic field ($\lvert H' \rvert$) observed from the Eyrewell (EYR) magnetometer was >40 nT/min. aa*, ap and Kp are global geomagnetic indices, while the EYR ak is the ak index derived from the Eyrewell magnetic observations. The two GIC columns are the magnitudes of the currents observed at the number 6 transformer at Islington substation (ISL M6) and the number 4 transformer at Halfway Bush substation (HWB T4), while Ratio is the ratio of the two GIC quantities (HWB T4/ISL M6). Complete data is only given for events when there are GIC observations at ISL M6.

#	Time [UT]	**60 s [nT/min]**	**20 s [nT/min]**	**5 s [nT/min]**	**1 s [nT/min]**	**ISL M6 GIC (A)**
1	6 Nov 2001 1:52	190.8	273.0	-	-	33.1
2	31 Oct 2003 5:36	170.6	-	297.8	-	21.1
3	29 Oct 2003 6:11	166.2	-	583.1	-	34.1
5	18 Feb 2003 5:08	109.4	-	347.5	-	12.5
6	15 May 2005 8:17	97.9	198.6	223.2	-	15.0
7	8 Nov 2004 7:12	90.2	111.9	-	-	14.9
8	29 May 2003 22:09	88.7	-	248.2	-	14.3
9	2 Oct 2013 1:56	85.6	-	-	165.0	19.1
10	20 Nov 2003 18:36	78.0	-	161.3	-	12.1
11	10 Nov 2004 2:42	74.9	-	-	-	14.2
12	4 Nov 2003 6:27	73.9	-	161.3	-	13.0
13	17 Mar 2015 4:46	68.6	-	-	246.7	17.0
14	23 Apr 2002 4:49	66.9	-	186.1	-	11.1
16	11 Sep 2005 5:37	62.6	245.1	295.2	-	19.2
18	21 Jan 2005 23:18	60.3	77.4	-	-	8.0
19	26 Jul 2004 22:50	57.6	328.8	-	-	18.6
21	5 Dec 2004 7:47	56.8	-	-	-	8.6
22	17 Mar 2013 6:01	54.3	-	-	228.2	13.2
23	24 Oct 2003 15:25	52.5	-	86.9	-	7.3
25	22 Jun 2015 18:34	51.2	-	-	237.5	12.2
26	17 Apr 2002 11:07	47.8	-	62.0	-	6.5
27	12 Sep 2014 15:55	43.3	-	-	82.0	9.8
28	9 May 2003 7:43	42.7	-	62.0	-	4.6
30	18 Mar 2002 13:23	41.6	-	62.0	-	5.9
31	26 Sep 2011 19:38	40.6	-	-	195.6	8.7

Table 2. Additional information on the EYR magnetic field observations of $|H'|$ for the events shown in Table 1. In all cases there are additional observations of the rate of change of the horizontal component of the magnetic field ($|H'|$) made at higher time resolution, either 20 s, 5 s, or 1 s resolution. Events have been included in the table only when there are GIC observations at ISL M6.

Figure 1. Map of the South Island of New Zealand showing the Transpower New Zealand electrical transmission network (colored lines). The heavy purple line is the HVDC line linking the South Island and North Island electrical networks. The other colored lines in this figure show the routes of the Transpower transmission lines, with different colors representing different voltages (orange = 220 kV, red = 110 kV, light blue = 50/66 kV). Stars show the location of the Islington and Halfway Bush substations. The location of the primary New Zealand magnetic observatory, Eyrewell, is given by the blue hexagon.

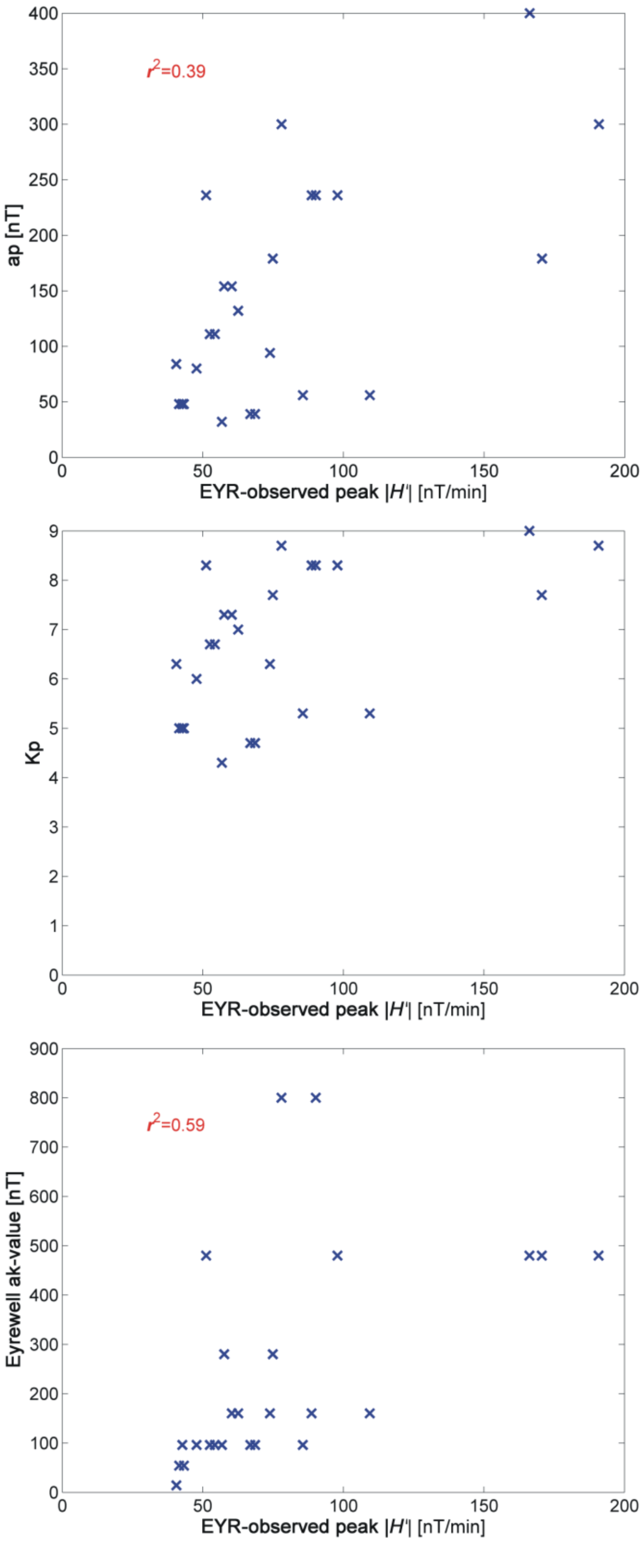

Figure 2. Comparison between geomagnetic index values and the peak |*H*′| value determined from the Eyrewell (EYR) magnetic observatory data. The upper two panels are the global indices ap and Kp, while the lower panel is the Eyrewell-derived ak-index.

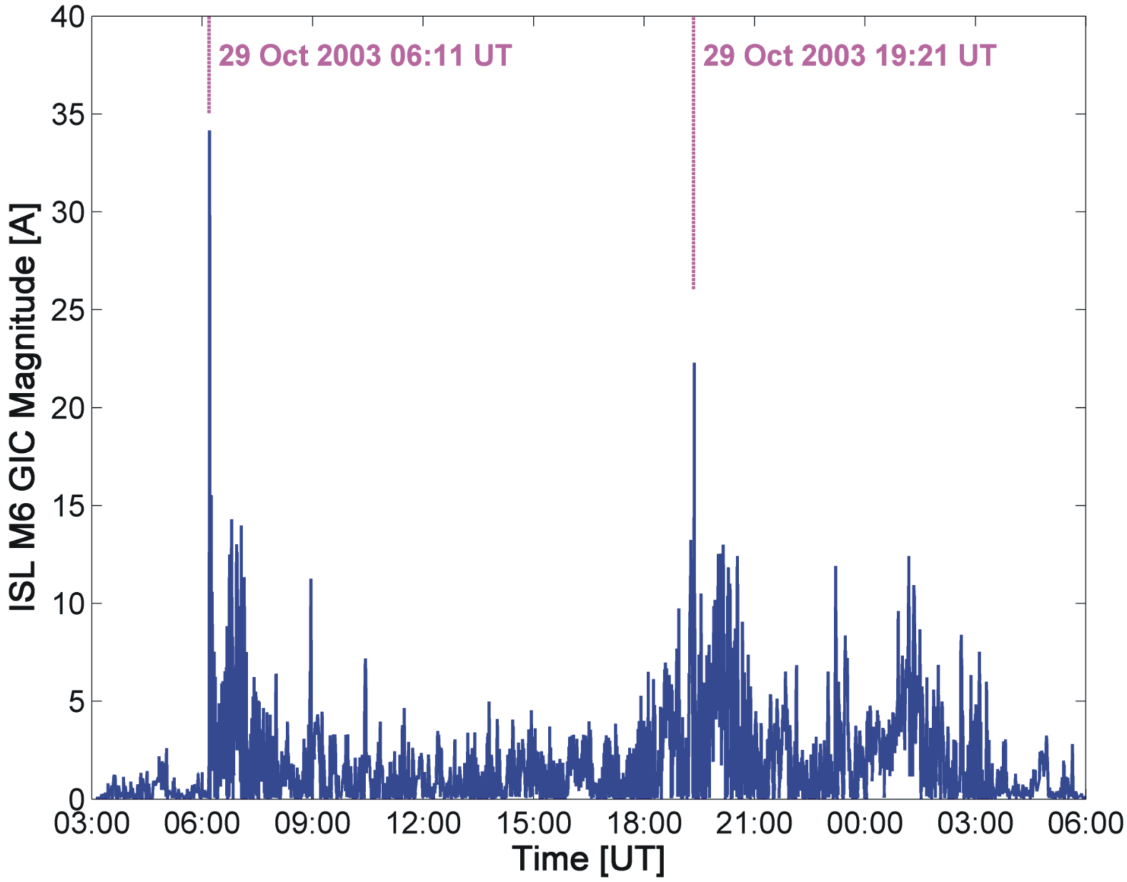

Figure 3. Time variation of GIC observed at the number 6 transformer at Islington substation (ISL M6) at the start of the 2003 Halloween storm. This began with a sudden storm commencement at 06:11 UT on 29 October 2003, as marked by the first magenta line. A second significant GIC impulse is marked at 19:21 UT.

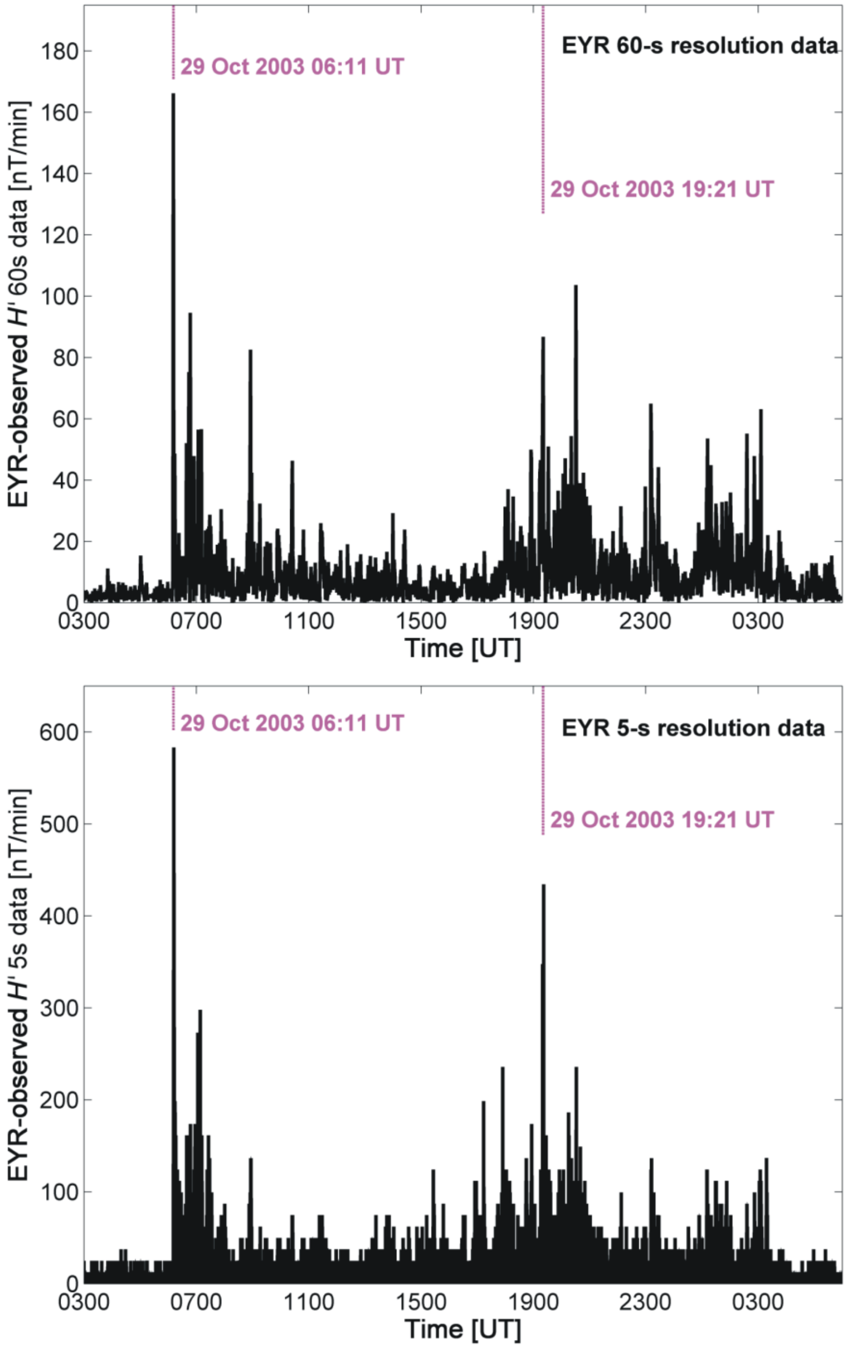

Figure 4. Time variation of $|H'|$ values derived from Eyrewell (EYR) magnetic observatory data at the start of the 2003 Halloween storm, in a format similar to Figure 3. The upper panel uses 60 s resolution magnetic field data, while the lower panel uses the 5 s data.

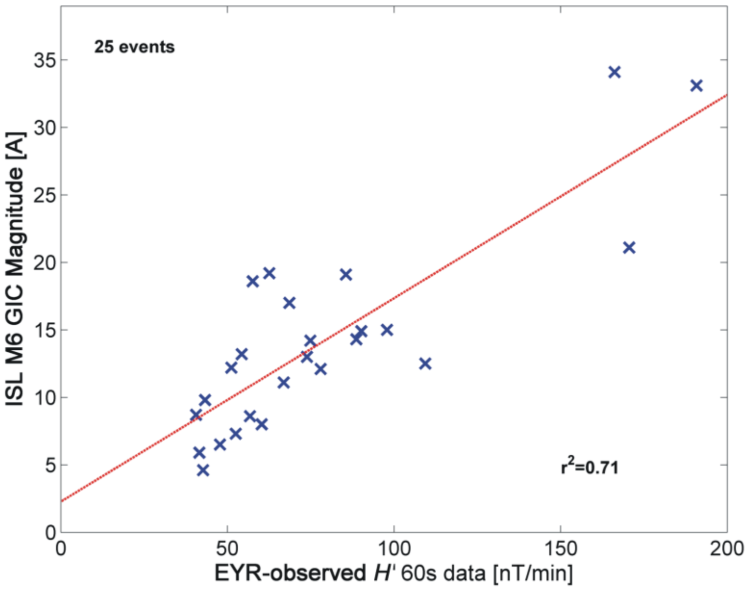

Figure 5. Comparison between the magnitude of the GIC observed at the number 6 transformer at Islington substation (ISL M6) with peak $|H'|$ values derived from 60 s Eyrewell (EYR) magnetic observatory data. The dashed red line is a linear fit to the 25 events.

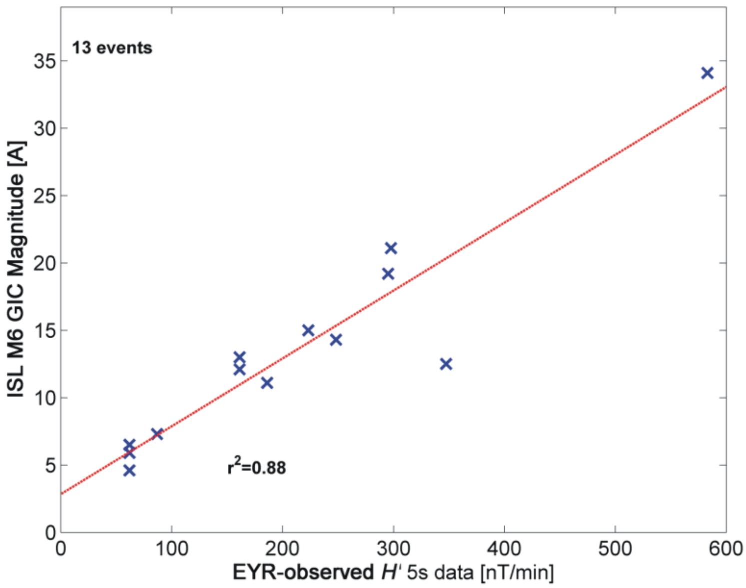

Figure 6. Comparison between the magnitude of the GIC observed at the number 6 transformer at Islington substation (ISL M6) with peak $|H'|$ values derived from 5 s Eyrewell (EYR) magnetic observatory data, in the same format as Figure 5.

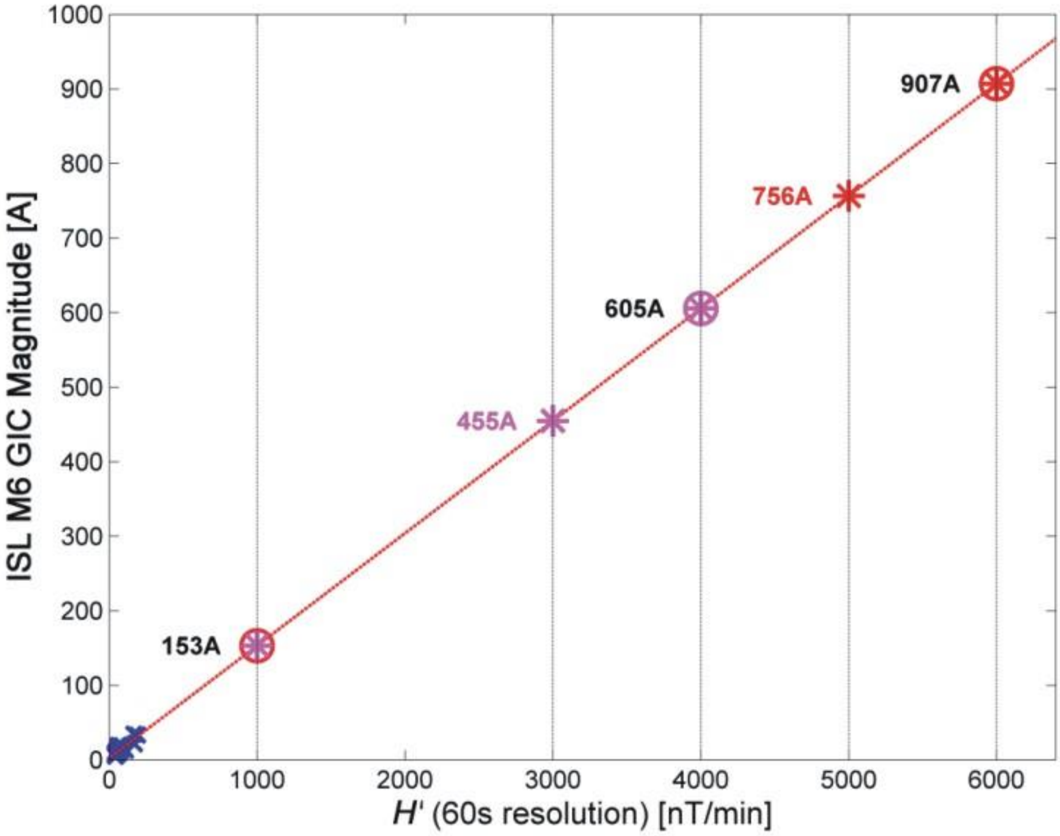

Figure 7. Estimates of the peak GIC predicted for transformer number 6 at the Islington substation (ISL M6) based on *H′* rates for extreme storms and an extrapolation from the fitting in Figure 5. Results for return periods of 100 years are shown by magenta stars, and 200 year return periods by red stars. The 95% confidence interval range is show by the ringed values (1000-4000 nT/min for 100 years and 1000-6000 nT/min for 200 years).

Figure 1.


From 2001 GIC-monitoring location
From 2012 GIC-monitoring location
Magnetometer location
Eyrewell
Islington
Halfway Bush
Motupipi
Upper Takaka
Cobb
Motueka
Fighting Bay
Stoke
Blenheim
Kikiwa
Argyle
Branch River
Waimangaroa
Orowaiti
Westport
Robertson Street
Murchison
Inangahua
Reefton
Blackwater
Atarau
Greymouth
Dobson
Kaikoura
Kumara
Kawhaka
Hokitika
Two Mile Road
Culverden
Otira
Arthur's Pass
Waipara
Castle Hill
Ashley
Southbrook
Kaiapoi
Coleridge
Papanui
Hororata
Bromley
Addington
Middleton
Brackendale
Ashburton
Tekapo A
Tekapo B
Twizel
Ohau A
Ohau B
Ohau C
Temuka
Albury
Timaru
Bog Roy
Benmore
Aviemore
Waitaki
Studholme
Bells Pond
Glenavy
Livingstone
Blackpoint
Frankton
Cromwell
Naseby
Oamaru
Clyde
Roxburgh
Palmerston
Manapouri
Three Mile Hill
Halfway Bush
South Dunedin
Waipori
Berwick
Gore
Balclutha
Brydone
North Makarewa
Edendale
Invercargill
Tiwai

Figure 2.

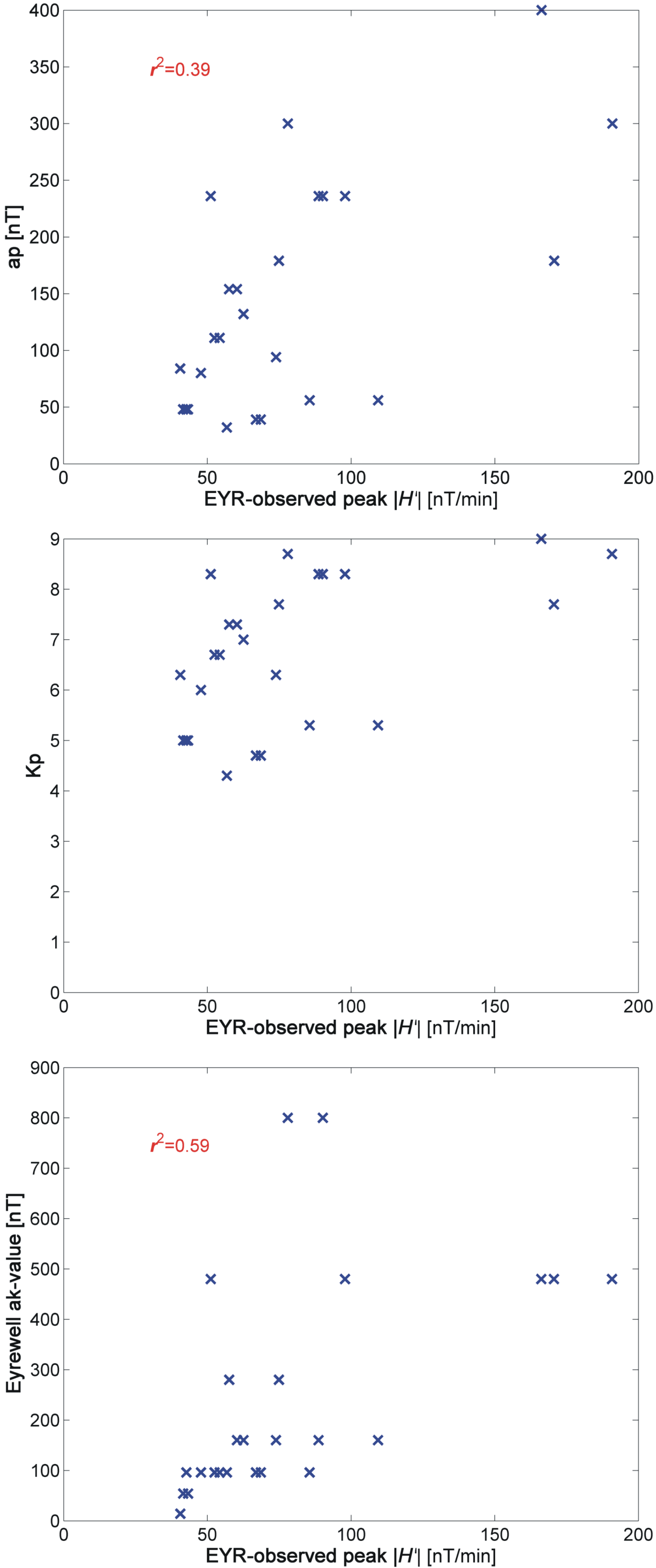

r²=0.39
ap [nT]
EYR-observed peak |H'| [nT/min]
Kp
EYR-observed peak |H'| [nT/min]
r²=0.59
Eyrewell ak-value [nT]
EYR-observed peak |H'| [nT/min]

Figure 3.

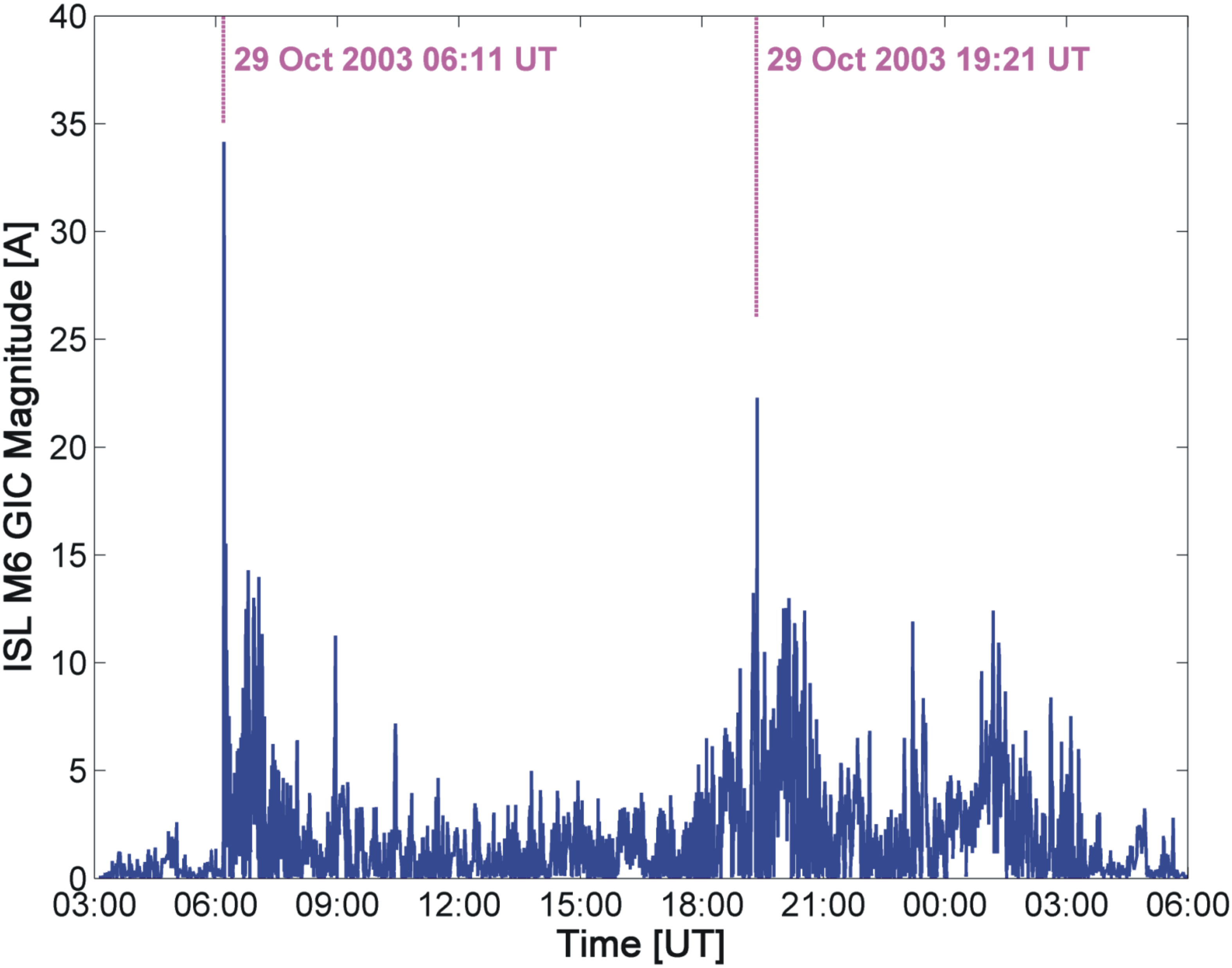

29 Oct 2003 06:11 UT
29 Oct 2003 19:21 UT
ISL M6 GIC Magnitude [A]
Time [UT]
0
5
10
15
20
25
30
35
40
03:00
06:00
09:00
12:00
15:00
18:00
21:00
00:00
03:00
06:00

Figure 4.

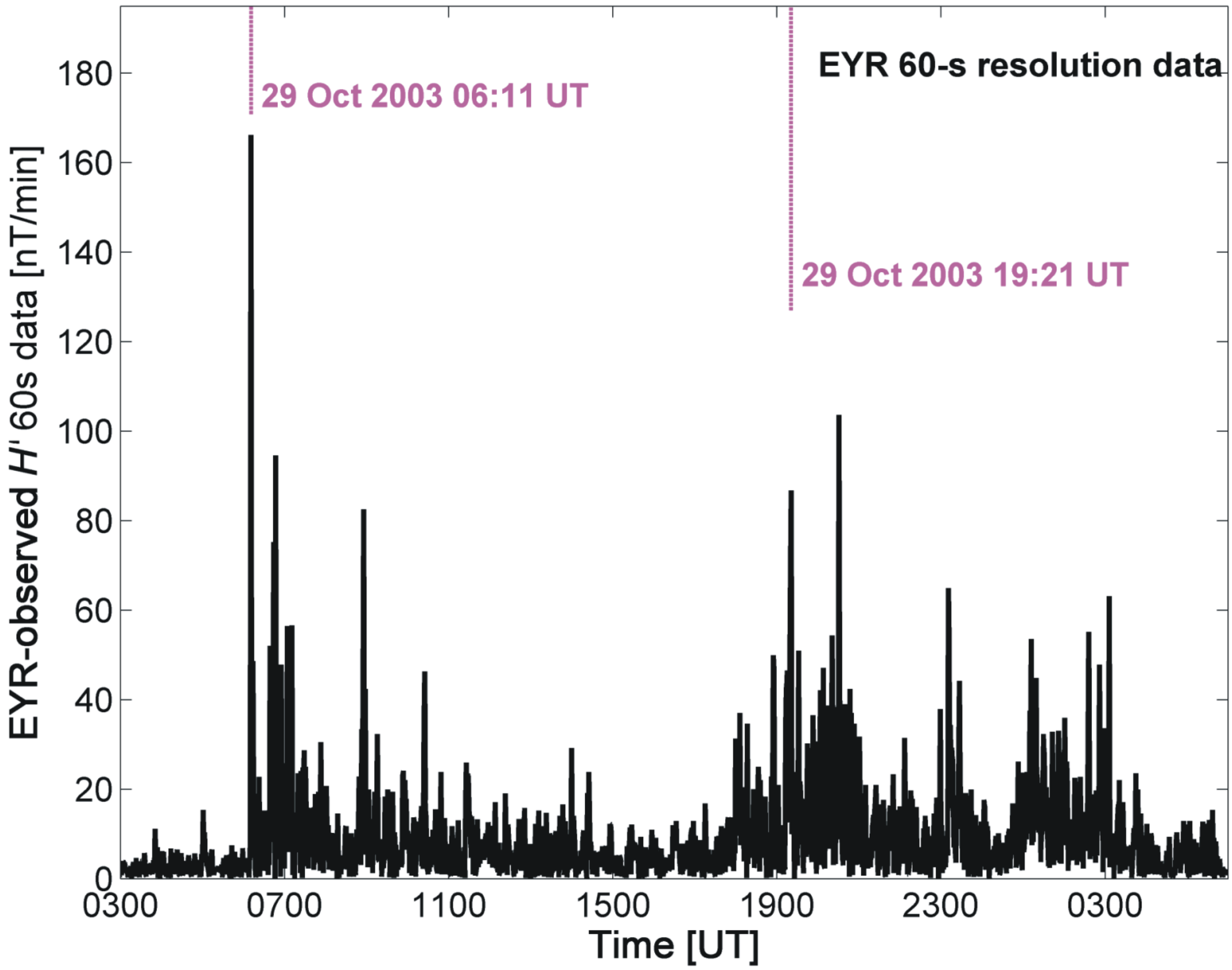

EYR 60-s resolution data
29 Oct 2003 06:11 UT
29 Oct 2003 19:21 UT
EYR-observed H' 60s data [nT/min]
0
20
40
60
80
100
120
140
160
180
0300
0700
1100
1500
1900
2300
0300
Time [UT]

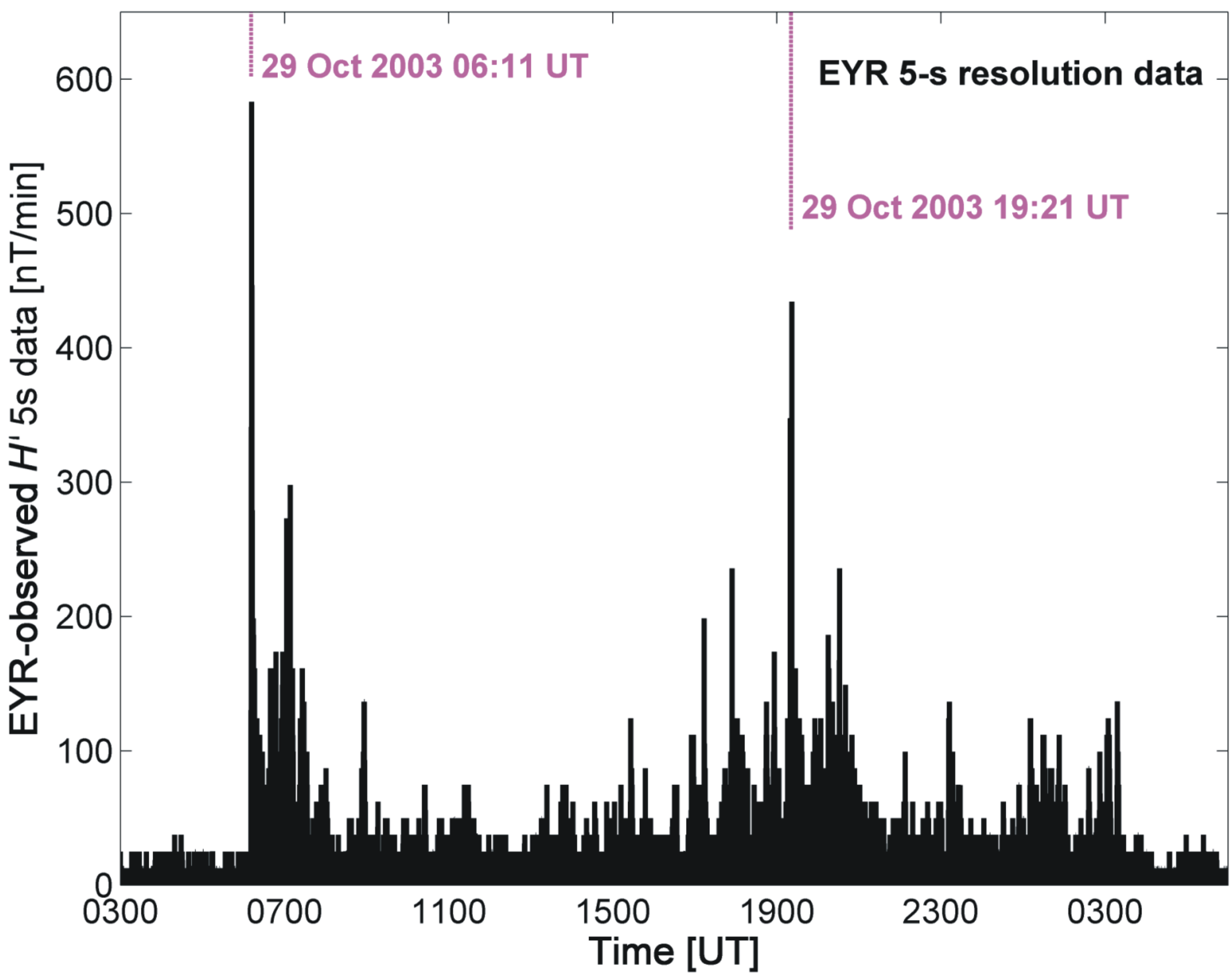

EYR 5-s resolution data
29 Oct 2003 06:11 UT
29 Oct 2003 19:21 UT
EYR-observed H' 5s data [nT/min]
0
100
200
300
400
500
600
0300
0700
1100
1500
1900
2300
0300
Time [UT]

Figure 5.

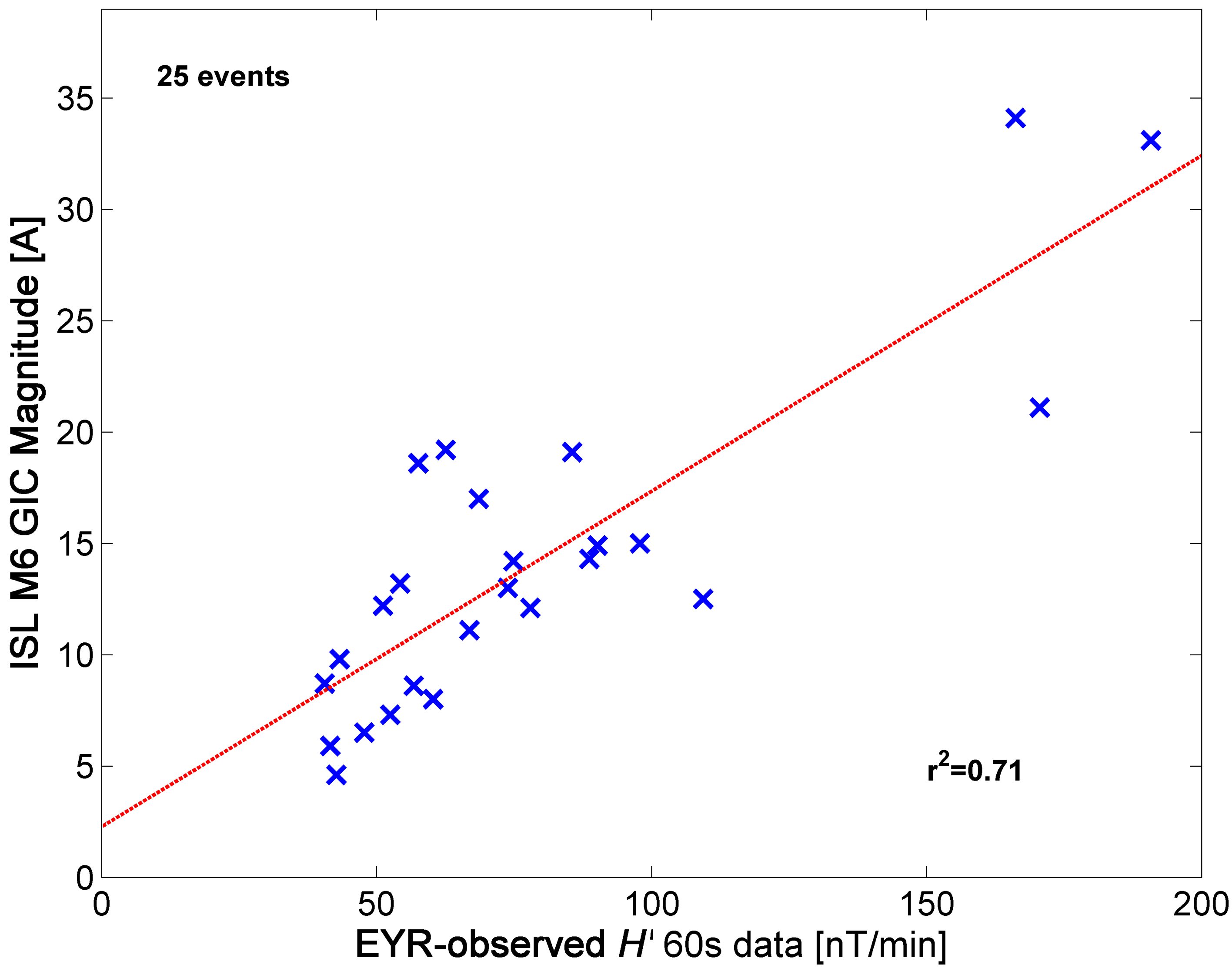
25 events
r²=0.71
ISL M6 GIC Magnitude [A]
EYR-observed H' 60s data [nT/min]
0
5
10
15
20
25
30
35
0
50
100
150
200

Figure 6.

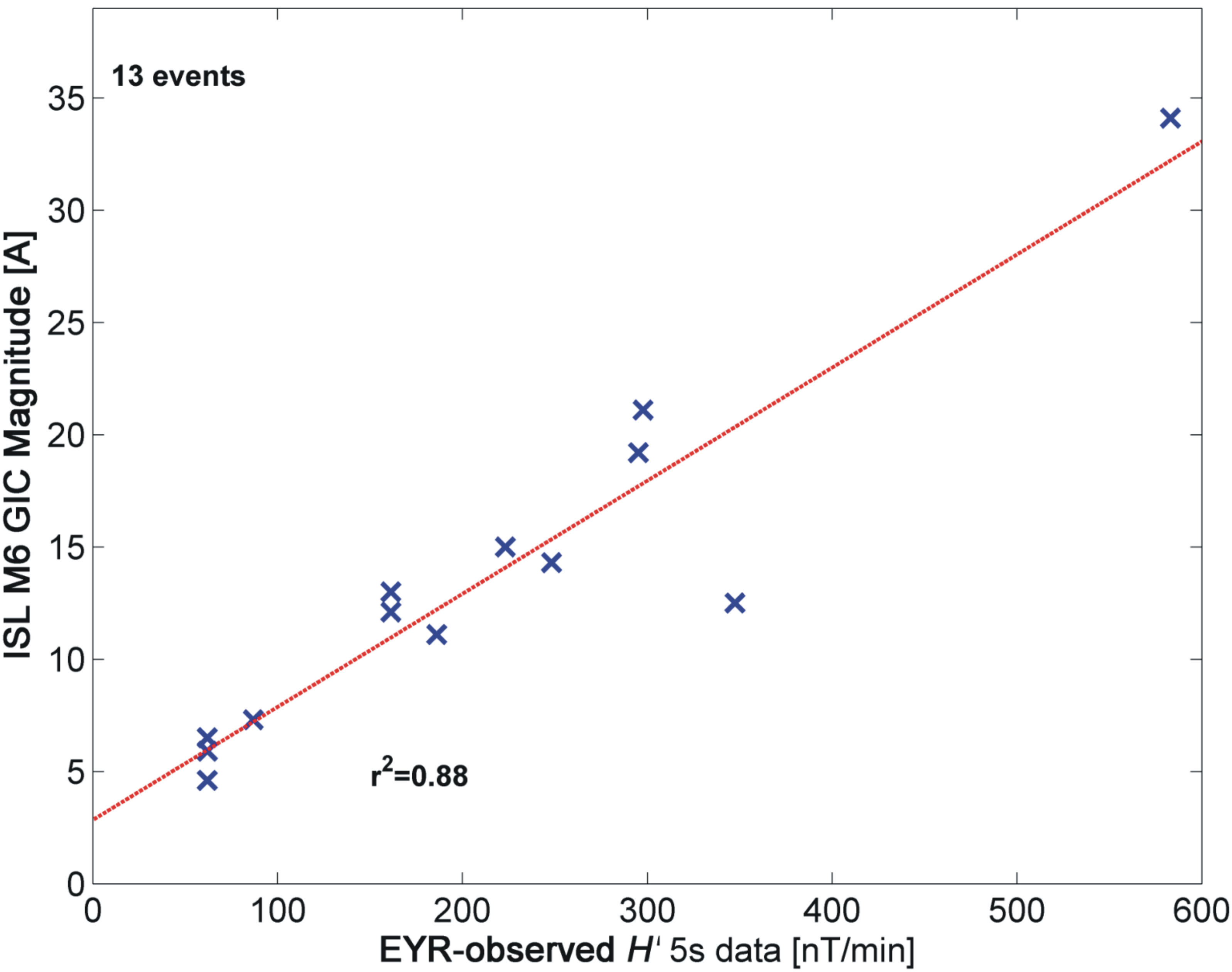
13 events
r^2=0.88
ISL M6 GIC Magnitude [A]
EYR-observed H' 5s data [nT/min]
0
5
10
15
20
25
30
35
0
100
200
300
400
500
600

Figure 7.

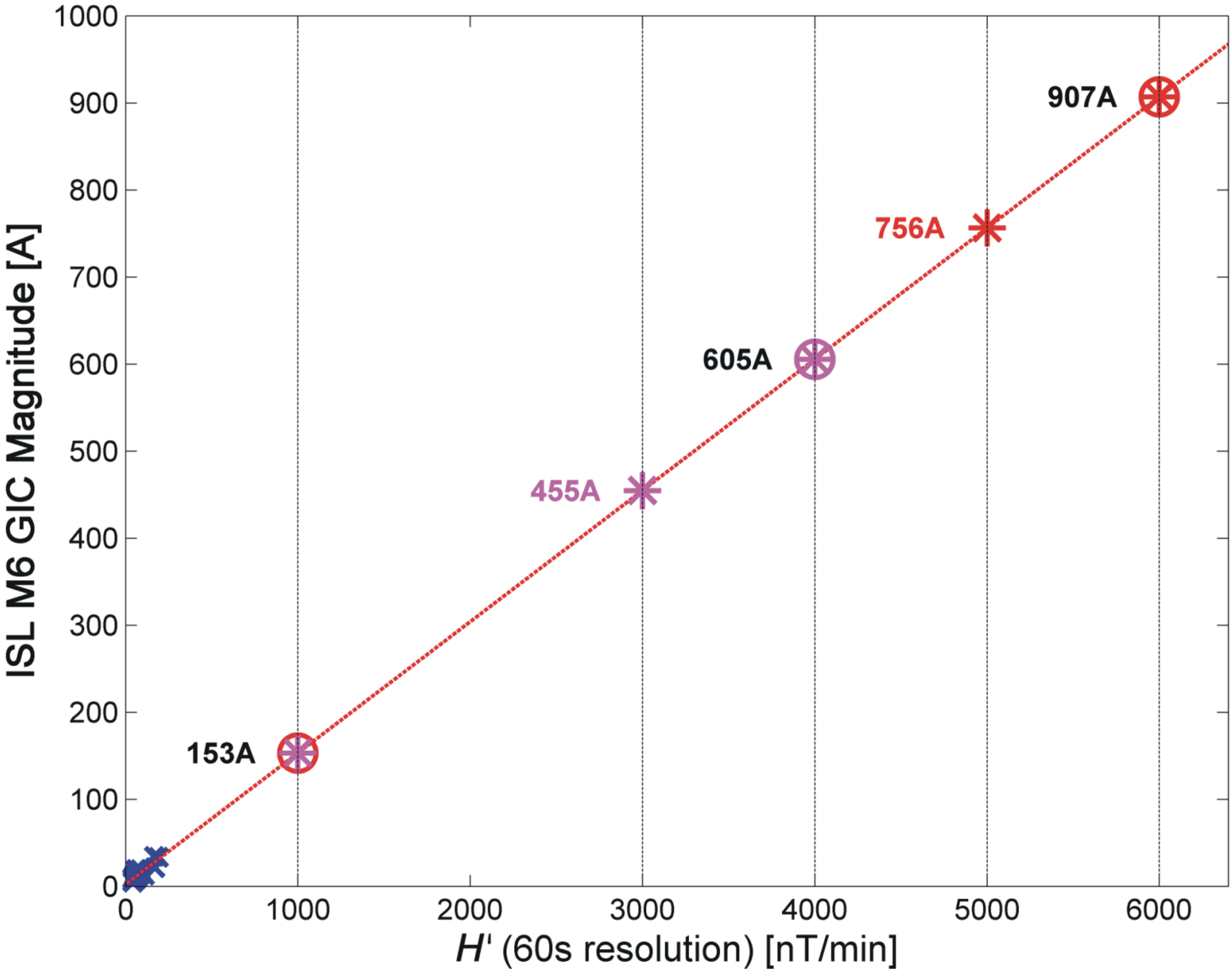

ISL M6 GIC Magnitude [A]
H' (60s resolution) [nT/min]
907A
756A
605A
455A
153A
0
100
200
300
400
500
600
700
800
900
1000
1000
2000
3000
4000
5000
6000